A wave solution for energy dissipation and exchange at nonclassical boundaries of a traveling string

E.W. Chen[a,*], J.F. Yuan[a], N.S. Ferguson[b],K. Zhang[a], W.D. Zhu[c], Y.M. Lu[a], H.Z. Wei[a]

[a]*School of Mechanical Engineering, Hefei University of Technology, Hefei, 230009, China*

[b]*Institute of Sound and Vibration Research, University of Southampton, Southampton SO171BJ, England, UK*

[c]*Department of Mechanical Engineering, University of Maryland, Baltimore County, Baltimore, MD 21250, USA*

Abstract

The finite length model of a traveling string can be used to study the lateral vibrations in many engineering devices. The vibrational energy exchange mechanism and its characteristics are very complex, due to the axial movement and the different boundary conditions. A finite length translating tensioned string model with mixed boundary conditions is considered here in order to study the exchange of vibrational energy during the reflection process. The boundary conditions are respectively at one end a spring-dashpot and the other a fixed boundary, together forming one kind of mixed boundary conditions. An analytical solution and energy expressions for the propagating wave are presented using a reflected wave superposition method. Firstly, a complete cycle of boundary reflections in the string is provided. To simplify the process for obtaining the response, each cycle is divided into three time intervals. Applying D'Alembert's principle and the reflection properties, expressions for the reflected waves under these mixed boundary conditions are derived with the vibrational response solved for three time intervals. The accuracy and efficiency of the proposed method are confirmed numerically by comparison to simulations produced using a Newmark-β method solution. The comparison shows that the reflected wave superposition method solution is achievable for higher translational speeds, even the critical speed, which is not attainable from most numerical methods. The subsequent energy analytical expressions for a traveling string with these mixed boundary conditions are obtained in terms of the superposition of the traveling waves and their reflections. The properties of vibration energy exchange as a function of the translational velocity, the type of boundary and level of damping are discussed. Numerical simulation results proved that the viscous damper results in energy dissipation at the boundary, and the choice of the magnitude and direction of the translational string velocity can affect the energy of the traveling wave.

Keywords: energy exchange; traveling string; nonclassical boundaries; reflection properties; wave superposition

1. Introduction

In the large number of present studies, most traveling string models fall into two categories: a semi-infinite or a finite length string model. Typically the two types of traveling string models have the uniform string density ρ, the traveling speed v and the

constant tension T. The finite string length model is more applicable for engineering applications. It can be used to study lateral vibrations in many practical devices (primarily for providing axial movement requirements), such as conveyor belts, elevator cables, mechanical power transmission belts, magnetic tapes and so on. Vibrational behavior, typically displacement and energy, is important for these systems, which have been studied for many years. The concept of wave propagation is used in this model, where wave reflections occur at both boundaries.

A large number of previous studies have examined the energy in representative string models. Miranker [1] found that the vibration energy of a tape moving between a pair of pulleys is not conserved, but transferred periodically into and out of the system. Any point on the traveling string experiences three acceleration components as seen by a stationary observer, i.e. the local acceleration, the Coriolis acceleration and the centripetal acceleration. Wickert and Mote [2] used the skew-symmetric principle for the equations of motion in a state space from to analyze the response problem for a traveling string and beam. Sack [3] used the harmonic response method to solve the forced response for a constant length string having a constant traveling speed. Zhu [4] distinguished the rates of change of energies of translating media from control volume and system viewpoints and established. Correspondences between translating media with variable length and stationary media with a moving boundary, and between translating media with constant length and stationary media with both boundaries moving at the same speed. Although the mechanical energy in an axially moving material is non-constant, Chen and Zhao [5] confirmed that there exists a conserved quantity in the free nonlinear transverse vibration of a translating beam constrained by simple or fixed supports. Lee and Mote [6] analyzed the energy of translating continua for fixed, free and damped boundary conditions. The main contributions of this paper is the evaluation of energy exchange using energy reflection coefficients defined by the boundary conditions. In particular, Chen and Ferguson [7] studied the energy dissipation by a viscous damper attached at one end of a moving string. The authors could obtain an optimum value for the damper which dissipates most input energy for a string with a constant or a varying length. In terms of dissipative boundaries, Gaiko and Van Horssen [8] also gave a complete and accurate description of the low frequency oscillatory behavior of the semi-infinite traveling string with an attached spring–dashpot system at one end. They obtained the response to the initial conditions using the method of D'Alembert. Chen et al.[9-11] investigated a reflected wave superposition method, which was proposed for a finite axially traveling string with classical and nonclassical boundaries at the two ends, and analyzed the total mechanical energy as well as its time rate of change. Huang et al.[12] investigated the dynamic responses of high-dimensional nonlinear models of a fixed-fixed translating beam, and analyzed continuous energy exchange and the beating waveform phenomenon of high-dimensional models. Chen et al.[13] adopted the complex mode theory to obtain modal components and subsequently the modal energy for a traveling string.

However, as for the relationship for the energy exchange occurring in the traveling string reflected at mixed boundaries, analytical works are seldom reported. In this study, based on the reflection equations at the spring-dashpot and fixed boundaries, a reflected wave superposition method is introduced and completely developed. The combination of

the incident and reflected waves at two ends of the string constitutes the resulting free vibration. This research provides an analytical way to study the mechanism of energy exchange of the translating medium defined over a finite domain with mixed boundary conditions.

This paper is organized as follows. Section 2 introduces the equation of motion describing the lateral vibration of an axially traveling finite string and the relevant boundary conditions. In Section 3, the reflected wave superposition method is used to obtain the response due to general initial displacement and velocity conditions of a string traveling between two types of boundaries separated by a constant distance, i.e. the length of string between the boundaries is constant. Next, Section 4 investigates the time varying cycle and gives an exact analytical response for the free vibration of the axially traveling finite string. In Section5, expression for the vibrational energy of the string with the dashpot-spring and fixed boundary conditions is obtained using the proposed reflected wave super position method. The total mechanical energy and its time rate of change are analyzed. Finally, Section 6 provides the main conclusions.

2. The governing equation of motion of a traveling string

Fig. 1 shows the traveling string system with one end supported by a spring and a viscous damper acting in parallel and the other end fixed, which are subsequently named as the spring-dashpot_fixed boundary conditions in this paper. In Fig.1, k is the stiffness of the spring, η is the viscous damping coefficient at the left boundary, and x is a fixed spatial coordinate system, which represents the axial position of a point in the string.

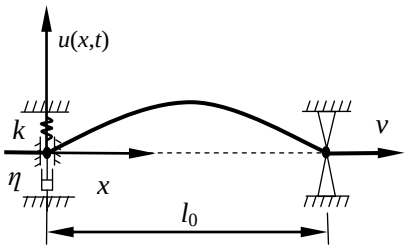

Fig. 1. Traveling string with spring-dashpot_fixed boundaries

One can obtain the governing equation of motion for the traveling string in Fig.1 by applying Hamilton's principle in the following form[14,15]

$$\int_{t_2}^{t_1}\left(\delta(E_k - E_p) + \delta W\right)\mathrm{d}t = 0 \tag{1}$$

where t_1 and t_2 are any two instants of time and δ is a variation of a function; E_k and E_p are the kinetic and potential energy, respectively; and δW is the virtual work done by the non-conservative damping force at the downstream boundary. The kinetic energy of the string E_k is given by

$$E_\mathrm{K} = \frac{1}{2}\int_0^{l_0} \rho\left[v^2 + (u_t + vu_x)^2\right]\mathrm{d}x \tag{2-1}$$

where l_0 is the length of the string, ρ is the uniform string mass per unit length and v is the constant translational speed of the string; $u(x, t)$ represents the transverse displacement of

the axial moving string at the coordinate x and the time t, so that $u_t = \partial u/\partial t$ and $u_x = \partial u/\partial x$; and $u_t + v u_x$ is the instantaneous transverse velocity of a material particle. The potential energy E_p comprises the work done by deflecting the string from its equilibrium position [8] and the work done by the linear spring at $x = 0$, which is given by

$$E_P = \frac{1}{2}\int_0^{l_0} T u_x^{\,2} \mathrm{d}x + \frac{1}{8}\int_0^{l_0} EA u_x^{\,4} \mathrm{d}x + \frac{1}{2} k u^2(0,t) \tag{2-2}$$

where E is the Young's modulus of the string, A is the cross-sectional area and T is the uniform tension of the string. The first term in Eq.(2-2) is due to the tension force T and the second term in Eq. (2-2) is due to the nonlinear geometric deformation, which produces the stretching of the string[7,16]. The virtual work δW due to the dashpot is given by

$$\delta W = -\eta u_t(0,t)\delta u(0,t) \tag{3}$$

Substituting Eqs. (2-1), (2-2) and (3) into Eq. (1), one obtains

$$\begin{aligned} &\frac{1}{2}\delta\int_{t_1}^{t_2}\left[\int_0^{l_0}\left(\rho v^2 + \rho(u_t + v u_x)^2 - T u_x^{\,2} - \frac{1}{4} EA u_x^{\,4}\right)\mathrm{d}x - k u^2(0,t)\right]\mathrm{d}t \\ &-\delta\int_{t_1}^{t_2} \eta u_t(0,t) u(0,t)\mathrm{d}t = 0 \end{aligned} \tag{4}$$

Applying integration by parts to Eq.(4) yields

$$\begin{aligned} &\int_{t_1}^{t_2}\int_0^{l_0}[\rho(u_{tt} + 2v u_{xt} + \dot{v} u_x + u_{xx} v^2) - (T u_{xx} + \frac{3}{4} EA u_x^{\,2} u_{xx})]\delta u \mathrm{d}x\mathrm{d}t - \\ &\int_{t_1}^{t_2}(\rho u_t v + \rho u_x v^2 - T u_x - \frac{1}{4} EA u_x^{\,3})\delta u\,|_0^{l_0}\,\mathrm{d}t - \int_{t_1}^{t_2}[k u(0,t) + \eta u_t(0,t)]\delta u(0,t)\mathrm{d}t = 0 \end{aligned} \tag{5}$$

The governing equation of motion is contained in the first term of Eq. (5), and it is given by

$$\rho(u_{tt} + 2v u_{xt} + \dot{v} u_x + u_{xx} v^2) - (T u_{xx} + \frac{3}{4} EA u_x^{\,2} u_{xx}) = 0 \tag{6}$$

The boundary conditions for force equilibrium are contained in the remaining two terms of Eq. (5), which are given by

$$\rho u_t(l_0,t)v + \rho u_x(l_0,t)v^2 - T u_x(l_0,t) - \frac{1}{4} EA u_x^3(l_0,t) = 0 \tag{6-1}$$

$$\rho u_t(0,t)v + \rho u_x(0,t)v^2 - T u_x(0,t) - \frac{1}{4} EA u_x^3(0,t) - k u(0,t) - \eta u_t(0,t) = 0 \tag{6-2}$$

Since the string is fixed at $x = l_0$ as shown in Fig.1, the geometric boundary conditions at $x = l_0$ is given as follows:

$$u(l_0,t) = 0 \tag{7}$$

Eq.(6-1) will be automatically guaranteed when substituting Eq. (7) into Eq. (6-1), so Eq.(7)is selected as the only boundary condition at $x = l_0$ for subsequent calculation

In order to simplify the modeling process, the following assumptions are made:

(1) The effects of longitudinal vibration of the moving string as well as the nonlinear

geometric deformation are neglected.

(2) The values for the translational speed, elastic modulus, cross sectional area, density and tension of the string are constants when the traveling string vibrates transversely.

(3) The string translational speed v is assumed to be less than the free wave propagation speed c, i.e. $|v| < c$, where $c = \sqrt{T/\rho}$, so that the moving waves can be transmitted outward in the string direction to avoid energy accumulation[6].

Thus the governing equation of motion can be simplified to

$$u_{tt} + 2vu_{xt} - \left(c^2 - v^2\right)u_{xx} = 0 \tag{8}$$

and the boundary conditions are rewritten as

$$\begin{cases} ku(0,t) + \eta u_t(0,t) = \rho v\left[u_t(0,t) + vu_x(0,t)\right] - Tu_x(0,t) \\ u(l_0,t) = 0 \end{cases} \tag{9}$$

The flow chart for the analytical derivation is shown in Fig. 2.

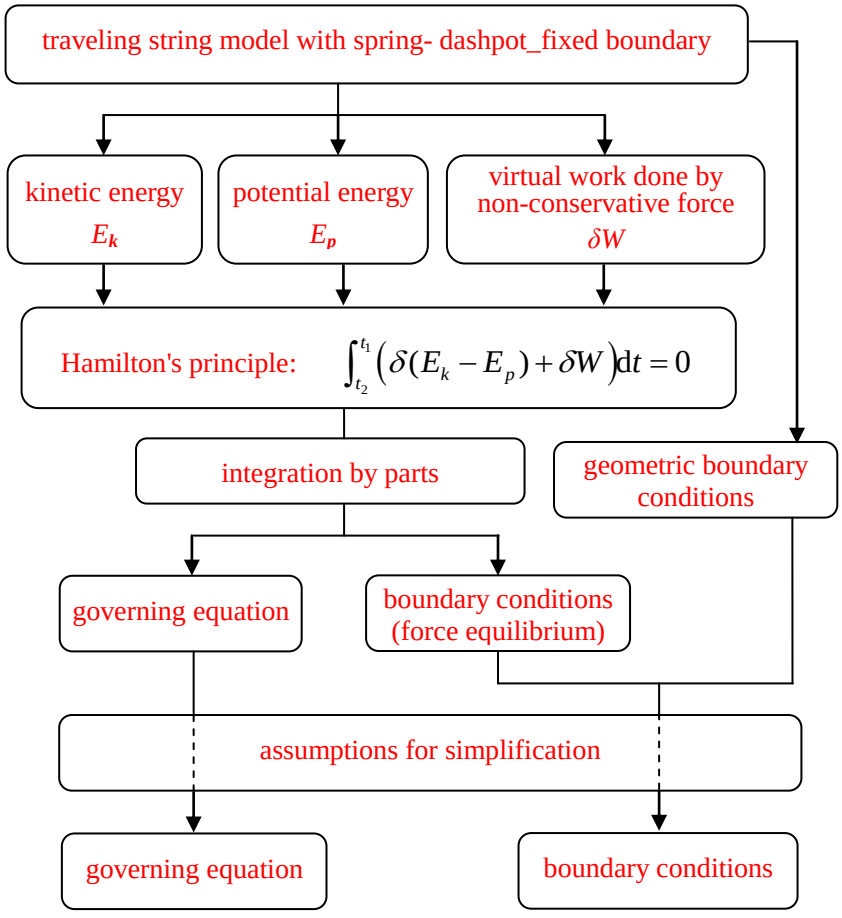

Fig. 2.Flow chart for the analytical derivation

3. Reflection equations at the boundaries

Using the D'Alembert method, the general one-dimensional wave solution of Eq. (8) is given by [17,18]:

$$u(x,t)=F(x-v_r t)+G(x+v_l t) \tag{10}$$

where $F(x - v_r t)$ is the right-propagating wave with speed of $v_r = c + v$ and $G(x + v_l t)$ is the left-propagating wave with speed of $v_l = c - v$, according to the fixed coordinate system.

The initial conditions for the string vibration are given as follows:

$$u(x,0)=\phi(x), 0\le x\le l_0 \tag{11-1}$$

$$u_t(x,0)=\psi(x), 0\le x\le l_0 \tag{11-2}$$

Substituting Eq. (10) into Eqs. (11-1) and (11-2), respectively, one obtains the expressions for $F(x)$ and $G(x)$ as follows:

$$\begin{cases} F(x)=\dfrac{v_l}{2c}\phi(x)-\dfrac{1}{2c}\int_0^x \psi(\xi)\,\mathrm{d}\xi - C \\ G(x)=\dfrac{v_r}{2c}\phi(x)+\dfrac{1}{2c}\int_0^x \psi(\xi)\,\mathrm{d}\xi + C \end{cases} \tag{12}$$

where C is a constant of integration.

According to Fig.1 and substituting Eq. (10) into the boundary condition of Eq. (9), one obtains the following equations:

$$G(l_0+v_l t)=-F(l_0-v_r t) \tag{13}$$

$$\begin{aligned} &k\left[F(-v_r t)+G(v_l t)\right]+\eta\left[-v_r F'(-v_r t)+v_l G'(v_l t)\right]= \\ &\rho v\left[-v_r F'(-v_r t)+v_l G'(v_l t)+vF'(-v_r t)+vG'(v_l t)\right]-T\left[F'(-v_r t)+G'(v_l t)\right] \end{aligned} \tag{14}$$

Introducing the following notations for convenience into Eq. (14)

$$\begin{cases} \alpha=-\dfrac{k}{\rho v c-\eta v_r+T} \\ \beta=\dfrac{\rho v c-\eta v_l-T}{\rho v c-\eta v_r+T} \end{cases} \tag{15}$$

one then has

$$F'(-v_r t)-\alpha F(-v_r t)=\beta G'(v_l t)+\alpha G(v_l t) \tag{16}$$

Defining $s = -v_r t$, the above form can be converted to

$$F'(s)-\alpha F(s)=\beta G'\left(-\frac{v_l}{v_r}s\right)+\alpha G\left(-\frac{v_l}{v_r}s\right) \tag{17}$$

By using the integrating factor $e^{-\alpha s}$, the integration for Eq. (17) yields

$$\int_0^x\left[F'(s)-\alpha F(s)\right]e^{-\alpha s}\mathrm{d}s=\int_0^x\left[\beta G'\left(-\frac{v_l}{v_r}s\right)+\alpha G\left(-\frac{v_l}{v_r}s\right)\right]e^{-\alpha s}\mathrm{d}s \tag{18}$$

Hence, one has the solution

$$F(x)=\left(F(0)+\beta\frac{v_r}{v_l}G(0)\right)\mathrm{e}^{\alpha x}-\beta\frac{v_r}{v_l}G\left(-\frac{v_l}{v_r}x\right)-\alpha\left(\beta\frac{v_r}{v_l}-1\right)\mathrm{e}^{\alpha x}\int_0^x G\left(-\frac{v_l}{v_r}s\right)\mathrm{e}^{-\alpha s}\mathrm{d}s \tag{19}$$

Finally, combining Eqs. (13) and (19), one has the equation for the boundary reflection relationships for the spring-dashpot_fixed boundary conditions:

$$\begin{cases} G_r(x)=-F_i\left(\dfrac{2c}{v_l}l_0-\dfrac{v_r}{v_l}x\right) \\ F_r(x)=\left(F_r(0)+\beta\dfrac{v_r}{v_l}G_i(0)\right)\mathrm{e}^{\alpha x}-\beta\dfrac{v_r}{v_l}G_i\left(-\dfrac{v_l}{v_r}x\right)-\alpha\left(\beta\dfrac{v_r}{v_l}-1\right)\displaystyle\int_0^x G_i\left(-\frac{v_l}{v_r}s\right)\mathrm{e}^{\alpha(x-s)}\mathrm{d}s \end{cases} \tag{20}$$

where F_i and G_i are the incident waves (i = 1, 2) and F_r and G_r are the reflected waves (r = i +1).

According to Eq. (20), one can obtain the amplitude ratio R of the reflection wave to the incident wave:

$$R=\frac{F_r(x)}{G_i(x)}=\frac{\left(F_r(0)+\beta\dfrac{v_r}{v_l}G_i(0)\right)\mathrm{e}^{\alpha x}-\beta\dfrac{v_r}{v_l}G_i\left(-\dfrac{v_l}{v_r}x\right)-\alpha\left(\beta\dfrac{v_r}{v_l}-1\right)\displaystyle\int_0^x G_i\left(-\frac{v_l}{v_r}s\right)\mathrm{e}^{\alpha(x-s)}\mathrm{d}s}{G_i(x)} \tag{20-1}$$

The amplitude ratio R approaches zero with α = 0 and β = 0, which can yield an optimal damping expression for elimination of vibration as follow:

$$\eta_{opt}=\frac{\rho vc-T}{v_l}=\sqrt{T\rho} \tag{20-2}$$

This means that the optimal value of the boundary damping is only related to the tension and the density of the string, but not to the translational velocity of the string.

4. Solution

4.1 The cycle for a propagating wave in a traveling string

The cycle for a propagating wave in a traveling string is defined as the time T_0 required for the original waveform to completely reflect at two boundaries and return to its initial

position on the traveling string,, which is given by [6]:

$$T_0 = \frac{l_0}{v_r} + \frac{l_0}{v_l} = \frac{2cl_0}{c^2 - v^2} \tag{21}$$

The cycleT_0 is divided into three time intervals: [0, t_a], [t_a, t_b] and [t_b, T_0]. Here, t_a is the time required for the point on the left end of F_1 to move from end A to B and t_b is the time required for the point on the right end of G_1 to move from B to A, when $v > 0$, as shown in Fig. 3(a). When $v < 0$, the definitions of t_a and t_b change with each other. The detailed expressions for t_a and t_b are given in Ref. [9].

Fig.3 shows the reflection process of the left-propagating waves G_i and the right-propagating waves F_i (i = 1, 2, 3) during these three time intervals. The analytical solutions for the vibration responses are given next for these three time intervals for the spring-dashpot_fixed boundary conditions.

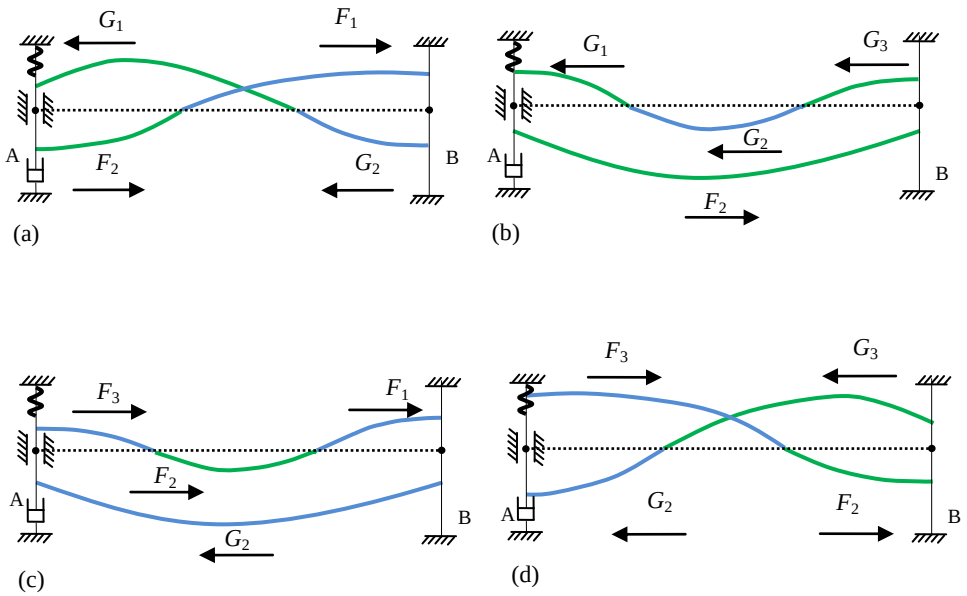

Fig.3.The propagating waves in a traveling string during three time intervals. (a) is for [0, t_a] and (d) is for [t_b, T_0] regardless of whether $v > 0$ or $v < 0$; (b) is for [t_a, t_b] when $v > 0$ and (c) is for [t_a, t_b] when $v < 0$. F_2 and G_2 are the reflection of waves G_1 and F_1; F_3 and G_3 are the reflection of waves G_2 and F_2.

4.2 Reflected wave superposition method

In this section the reflected wave superposition method is introduced to obtain the vibration response of the axial traveling string system. It uses the following three steps according to the division of the boundary reflection process in a single cycle.

4.2.1 $0 < t < t_a$

According to Eq.(12), the expressions for initial traveling wave F_1 and G_1 are

$$\begin{cases} F_1(x-v_r t)=\dfrac{v_l}{2c}\phi(x-v_r t)-\dfrac{1}{2c}\int_0^{x-v_r t}\psi(\xi)\,\mathrm{d}\xi-C \\ G_1(x+v_l t)=\dfrac{v_r}{2c}\phi(x+v_l t)+\dfrac{1}{2c}\int_0^{x+v_l t}\psi(\xi)\,\mathrm{d}\xi+C \end{cases} \tag{22}$$

In this time interval as shown in Fig.3(a), G_2 is the reflected wave of F_1 at the right-side boundary. Using the equation of boundary reflection Eq.(20), one has

$$G_2(x+v_l t)=-F_1\left(\frac{2c}{v_l}l_0-\frac{v_r}{v_l}\left(x+v_l t\right)\right) \tag{23}$$

The wave F_2 is the reflected wave of G_1 at the left-side boundary. Using the equation for the boundary reflection Eq.(20), one has

$$\begin{aligned} F_2\left(x-v_r t\right)=&\left(F_2\left(0\right)+\beta\frac{v_r}{v_l}G_1\left(0\right)\right)\mathrm{e}^{\alpha(x-v_r t)}-\beta\frac{v_r}{v_l}G_1\left(-\frac{v_l}{v_r}\left(x-v_r t\right)\right)- \\ &\alpha\left(\beta\frac{v_r}{v_l}-1\right)\int_0^{x-v_r t}G_1\left(-\frac{v_l}{v_r}s\right)\mathrm{e}^{\alpha(x-v_r t-s)}\mathrm{d}s \end{aligned} \tag{24}$$

Then applying the continuity condition that the value of traveling wave F_2 is the same as that of F_1 at the beginning of the reflection at the left boundary, i.e. $x = 0$, $t = 0$, one has

$$F_2\left(0\right)=F_1\left(0\right)=\frac{v_l}{2c}\phi\left(0\right) \tag{25}$$

From Eq. (12), $G_1(0)$ in Eq.(24) has the detailed expression as follows:

$$G_1(0)=\frac{v_r}{2c}\phi\left(0\right) \tag{26}$$

By substituting Eq. (25) into Eq. (24), the expression for F_2 can be obtained as follows:

$$\begin{aligned} F_2\left(x-v_r t\right)=&\left(F_1\left(0\right)+\beta\frac{v_r}{v_l}G_1\left(0\right)\right)\mathrm{e}^{\alpha(x-v_r t)}-\beta\frac{v_r}{v_l}G_1\left(-\frac{v_l}{v_r}\left(x-v_r t\right)\right)- \\ &\alpha\left(\beta\frac{v_r}{v_l}-1\right)\int_0^{x-v_r t}G_1\left(-\frac{v_l}{v_r}s\right)\mathrm{e}^{\alpha(x-v_r t-s)}\mathrm{d}s \end{aligned} \tag{27}$$

Hence, one has the expressions:

$$F\ (x-v_r t)=\begin{cases} F_1(x-v_r t)\,, & v_r t<x<l_0 \\ F_2(x-v_r t)\,, & 0<x<v_r t \end{cases} \tag{28}$$

$$G\ (x+v_l t)=\begin{cases} G_1(x+v_l t)\,, & 0<x<l_0-v_l t \\ G_2(x+v_l t)\,, & l_0-v_l t<x<l_0 \end{cases} \tag{29}$$

Finally, the expressions for the general solution of the equation of motion is

$$u\left(x,t\right)=F\left(x-v_r t\right)+G\left(x+v_l t\right),\ 0<t<t_a \tag{30}$$

4.2.2 $t_a < t < t_b$

If $v > 0$, one can see that the left end of F_1 disappears at the right boundary and G_3 is the reflected wave of F_2 at the right boundary, as shown in Fig. 3(b). Using Eq.(20), one has

$$G_3\left(x+v_l t\right)=-F_2\left(\frac{2c}{v_l}l_0-\frac{v_r}{v_l}\left(x+v_l t\right)\right) \tag{31}$$

Substituting Eq. (27) into Eq. (31), the expression for G_3 can be obtained as follows:

$$\begin{aligned} G_3\left(x+v_l t\right)&=-F_2\left(\frac{2c}{v_l}l_0-\frac{v_r}{v_l}\left(x+v_l t\right)\right)\\ &=-\left(F_1(0)+\beta\frac{v_r}{v_l}G_1(0)\right)\mathrm{e}^{\alpha\left(\frac{2c}{v_l}l_0-\frac{v_r}{v_l}\left(x+v_l t\right)\right)}+\beta\frac{v_r}{v_l}G_1\left(-\frac{2c}{v_r}l_0+x+v_l t\right)+\\ &\quad\alpha\left(\beta\frac{v_r}{v_l}-1\right)\int_0^{\frac{2c}{v_l}l_0-\frac{v_r}{v_l}\left(x+v_l t\right)}G_1\left(-\frac{v_l}{v_r}s\right)\mathrm{e}^{\alpha\left(\frac{2c}{v_l}l_0-\frac{v_r}{v_l}\left(x+v_l t\right)-s\right)}\mathrm{d}s \end{aligned} \tag{32}$$

In summary, one has the expressions:

$$F\left(x-v_r t\right)=F_2(x-v_r t),\ v_r t-\frac{v_r}{v_l}l_0<x<v_r t, v<0 \tag{32-1}$$

$$G\left(x+v_l t\right)=\begin{cases} G_1(x+v_l t),\ 0<x<l_0-v_l t, v>0\\ G_2(x+v_l t),\ l_0-v_l t<x<\dfrac{2cl_0}{v_r}-v_l t, v>0\\ G_3(x+v_l t),\ \dfrac{2cl_0}{v_r}-v_l t<x<l_0, v>0 \end{cases} \tag{32-2}$$

Finally, the expressions of the general solution of the equation of motion is

$$u\left(x,t\right)=F\left(x-v_r t\right)+G\left(x+v_l t\right),\ t_a<t<t_b \tag{32-3}$$

4.2.3 $t_b < t < T_0$

In this time interval as shown in Fig. 3(d), one can see that the right end of G_1 disappears at the left boundary and F_3 is the reflected wave of G_2 at the left boundary. Using Eq.(20), one has

$$\begin{aligned} F_3\left(x-v_r t\right)&=\left(F_3(0)+\beta\frac{v_r}{v_l}G_2(0)\right)\mathrm{e}^{\alpha\left(x-v_r t\right)}-\beta\frac{v_r}{v_l}G_2\left(-\frac{v_l}{v_r}\left(x-v_r t\right)\right)-\\ &\quad\alpha\left(\beta\frac{v_r}{v_l}-1\right)\int_0^{x-v_r t}G_2\left(-\frac{v_l}{v_r}s\right)\mathrm{e}^{\alpha\left(x-v_r t-s\right)}\mathrm{d}s \end{aligned} \tag{33}$$

From Eq. (23), one has

$$G_2(0)=-\frac{v_l}{2c}\phi\left(\frac{2c}{v_l}l_0\right)+\frac{1}{2c}\int_0^{\frac{2c}{v_l}l_0}\psi(\xi)\,\mathrm{d}\xi+C \tag{34}$$

The continuity condition for waves F_2 and F_3 is

$$F_3(0,\ t_b)=F_2(0,\ t_b) \tag{35}$$

Substituting Eqs. (24) and (33) into Eq. (35), one has

$$F_3(0)=F_2(0)+\beta\frac{v_r}{v_l}\left[G_1(0)\text{-}G_2(0)\right]-\beta\frac{v_r}{v_l}\left[G_1(v_lt_b)\text{-}G_2(v_lt_b)\right]\mathrm{e}^{v_rt_b\alpha}+ \alpha\left(\beta\frac{v_r}{v_l}-1\right)\int_{-v_rt_b}^{0}\left[G_1\left(-\frac{v_l}{v_r}s\right)\text{-}G_2\left(-\frac{v_l}{v_r}s\right)\right]\mathrm{e}^{-\alpha s}\mathrm{d}s+C \tag{36}$$

By substituting Eqs. (34) and (36) into Eq. (33), the expression for F_3 can be obtained as follows:

$$F_3\left(x-v_rt\right)=\left(\begin{array}{l} F_2(0)+\beta\frac{v_r}{v_l}\left[G_1(0)\text{-}G_2(0)\right]- \\ \beta\frac{v_r}{v_l}\left[G_1(v_lt_b)\text{-}G_2(v_lt_b)\right]\mathrm{e}^{v_rt_b\alpha}+ \\ \alpha\left(\beta\frac{v_r}{v_l}-1\right)\int_{-v_rt_b}^{0}\left[G_1\left(-\frac{v_l}{v_r}s\right)\text{-}G_2\left(-\frac{v_l}{v_r}s\right)\right]\mathrm{e}^{-\alpha s}\mathrm{d}s+ \\ \beta\frac{v_r}{v_l}\left[-\frac{v_l}{2c}\phi\left(\frac{2c}{v_l}l_0\right)\right] \end{array}\right)\mathrm{e}^{\alpha\left(x-v_rt\right)} -\beta\frac{v_r}{v_l}G_2\left(-\frac{v_l}{v_r}\left(x-v_rt\right)\right)-\alpha\left(\beta\frac{v_r}{v_l}-1\right)\int_0^{x-v_rt}G_2\left(-\frac{v_l}{v_r}s\right)\mathrm{e}^{\alpha\left(x-v_rt-s\right)}\mathrm{d}s \tag{37}$$

One has the expressions:

$$F\left(x-v_rt\right)=\begin{cases}F_2(x-v_rt)\,,\ v_rt-\frac{v_r}{v_l}l_0<x<l_0\\ F_3(x-v_rt)\,,\ 0<x<v_rt-\frac{v_r}{v_l}l_0\end{cases} \tag{37-1}$$

$$G\left(x+v_lt\right)=\begin{cases}G_2(x+v_lt)\,,\ \ 0<x<\frac{2cl_0}{v_r}-v_lt\\ G_3(x+v_lt)\,,\ \ \frac{2cl_0}{v_r}-v_lt<x<l_0\end{cases} \tag{37-2}$$

Finally, the expressions for the general solution of the equation of motion is

$$u\left(x,t\right)=F\left(x-v_rt\right)+G\left(x+v_lt\right),\ t_b<t<T_0 \tag{37-3}$$

When the string is translating to the left, i.e. $v<0$, $t_a<t<t_b$, as shown in Fig. 3(c), one can see that the left end of G_1 disappears at the left boundary and G_2 is the reflected wave of F_3 at the left boundary. The expressions for the propagating waves F_1, F_2, F_3 and G_2 are the same as the previous ones except for the different ranges of values of x.

4.3 Numerical simulation

Considering the continuity and the first order smoothness, the initial conditions for the numerical simulations are chosen as shown below:

$$\begin{cases} \psi(x) = 0 \\ \phi(x) = \left[H(x) - H(x - l_0) \right] A_0 \left[\sin \dfrac{\pi x}{l_0} \sin \dfrac{\pi (x - l_0)}{l_0} \right]^2 \end{cases} \tag{38}$$

where H is the Heaviside step function and $A_0$is amplitude of the incident wave.

The plots in Fig.4 show dimensionless displacement shape of the traveling string with the spring-dashpot_fixed boundary conditions using the proposed method, which compares with numerical solutions of a finite element model solved using the Newmark-β method[7].The parameters for the system are selected as follows: an amplitude A_0 = 0.01m, the length of string is l_0 = 3m, the linear viscous damping coefficient is η = 0.7Ns/m, the stiffness is k = 3 N/m, the string mass per unit length is 0.06 kg / m, the static uniform tension is T = 5 N and the dimensionless traveling speed is $V = v / c$.

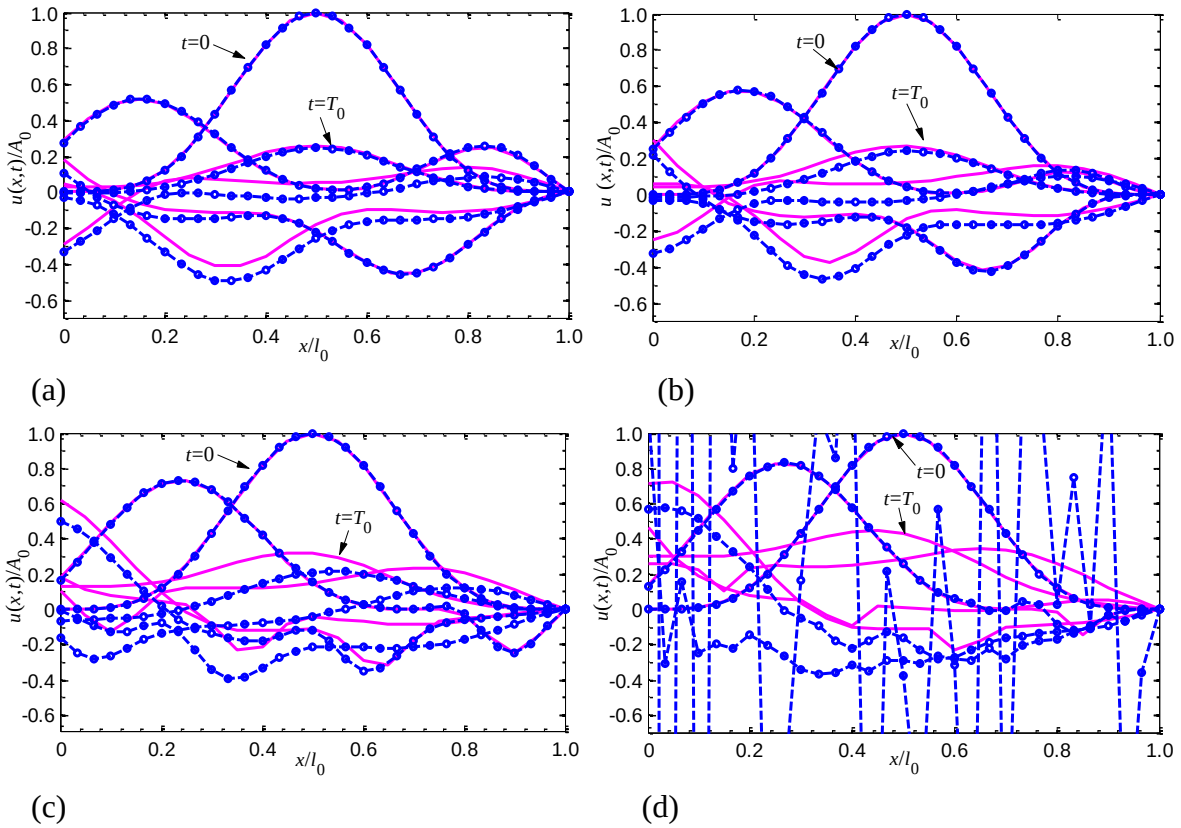

Fig. 4. Dimensionless displacement free transverse vibration response with spring-dashpot_fixed boundary over one period T_0 at the dimensionless traveling speeds of (a) V = 0.1, (b) V = 0.2, (c) V = 0.5 and (d) V = 0.7. The curves are identified by: —— wave superposition method; -○○○- Newmark-β method.

From Fig. 4 (a) to (c), one can see that the results of the two methods are basically the same at the lower translational moving string speed(i.e. V = 0.1, 0.2 and 0.5), at which the

Newmark-β method is still convergent. When the traveling speed is close to the critical speed c in Fig. 4(d) (V= 0.7), the wave superposition method is stable while the Newmark-β method has begun to diverge. Considering these cases, it can be surmised that the wave superposition method is suitable for a higher translational speed, even critical speed, which is not applicable to most numerical methods.

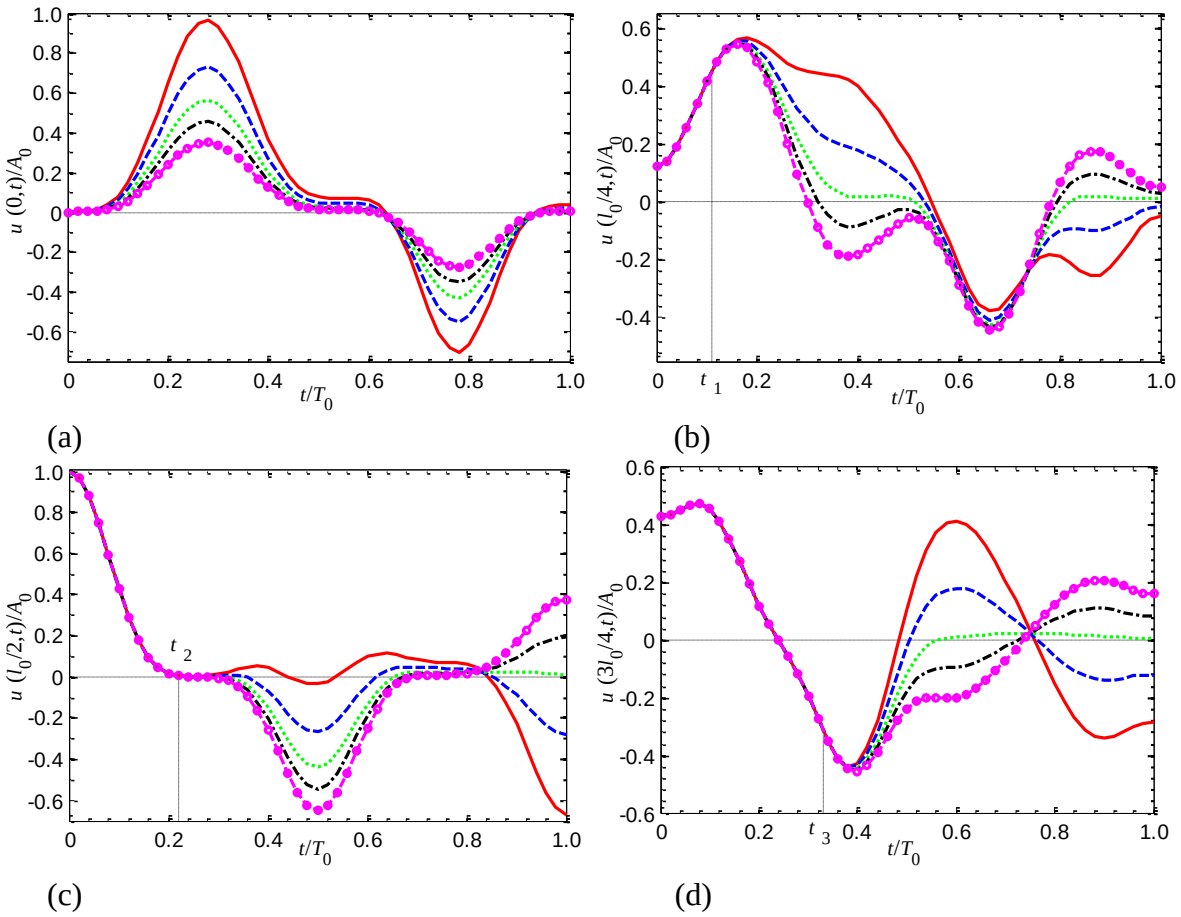

Fig. 5. Dimensionless displacement free transverse vibration response with spring-dashpot_fixed boundary over one period T_0 at different location of x. (a) x = 0, (b) x = 0.25L, (c) x = 0.5L, (d) x = 0.75L. The curves are identified by: — η = 0.1 Ns/m, -- η = 0.3 Ns/m, ---η = 0.55 Ns/m, ——η = 0.8 Ns/m, ○○○η = 1.2 Ns/m.

In Fig. 5, dimensionless displacement free transverse vibration response of some fixed coordinate position (x = 0, 0.25 l_0, 0.5 l_0 and 0.75 l_0) are given, which has different damping values (η = 0.1 Ns/m, 0.3 Ns/m, 0.55 Ns/m, 0.8 Ns/m and 1.2 Ns/m) over one period T_0 of the free vibration. Other parameters are the same as above except that the dimensionless traveling speed is V = 0.1. Fig. 5(a) shows that the free transverse vibration at the left boundary (x = 0) returns to the original position after a period T_0. One can also find that the free transverse vibration at the boundary(x = 0) is an equal-amplitude vibration about the x-axis. From Figs. 5(b) to (d), the amplitude of free transverse vibration response decreases as the damping value increase, clearly observed at the end of one period T_0.

When the damping value increases beyond the optimal damping value (η_{opt} = 0.55 Ns/m) obtained from Eq. (20-2), the phase of the displacement response will change at the

end of a period. For the damping value set equal to the optimal damping value, the amplitude of the free transverse vibration response will be reduced to zero at the end of the period T_0.

In Figs.5 (b) to (d), five curves overlap completely in the time interval of (0, t_1), (0, t_2) and (0, t_3)respectively, because the reflected waves, i.e. F_2 in Fig. 3(a), that attenuated at the left boundary have not yet reached the respective coordinate position(x = 0, x = 0.25 l_0, x = 0.5 l_0 and x = 0.75 l_0). Here the dimensionless times are $t_1 = 0.25\ l_0 / (T_0 v_r) = 0.11$, $t_2 = 0.5\ l_0 / (T_0 v_r) = 0.22$ and $t_3 = 0.75\ l_0 / (T_0 v_r) = 0.33$.

5 Vibrational energy

In this section, the vibrational energy for the traveling string with the spring-dashpot_fixed boundary is obtained based on the proposed reflected wave superposition method. The relationships between the energy and translational velocity of the string are also discussed.

When the spring–dashpot_fixed system is attached to the boundary, there is an additional contribution of potential energy of the spring $E_k(t)=\frac{1}{2}ku^2(0,t)$ to the total energy of the string system [19]:

$$E(t)=\frac{\rho}{2}\int_0^{l_0}\left[(u_t+vu_x)^2+c^2u_x{}^2\right]\mathrm{d}x+\frac{1}{2}ku^2(0,t) \tag{39}$$

From Eq. (10), one obtains

$$\begin{cases} u_t=-v_rF'+v_lG' \\ u_x=F'+G' \end{cases} \tag{39-1}$$

Incorporating Eqs. (39-1) and (10) into Eq. (39), one has

$$\begin{aligned} E(t)&=\frac{\rho}{2}\int_0^{l_0}\left[(-v_rF'+v_lG'+vF'+vG')^2+c^2(F'+G')^2\right]\mathrm{d}x+\frac{1}{2}ku^2(0,t) \\ &=\rho c^2\int_0^{l_0}(F'^2+G'^2)\,\mathrm{d}x+\frac{1}{2}k\left[F(0,t)+G(0,t)\right]^2 \end{aligned} \tag{40}$$

5.1 Vibrational energy expressions for the propagating waves

Taking the derivative of Eq. (27), one has

$$F_2'(x-v_rt)=\left\{\begin{array}{r}\left(F_1(0)+\beta\frac{v_r}{v_l}G_1(0)\right)\mathrm{e}^{\alpha(x-v_rt)}-\beta\frac{v_r}{v_l}G_1\left(-\frac{v_l}{v_r}x+v_lt\right)- \\ \alpha\left(\beta\frac{v_r}{v_l}-1\right)\mathrm{e}^{\alpha(x-v_rt)}\int_0^{x-v_rt}G_1\left(-\frac{v_l}{v_r}s\right)\mathrm{e}^{-\alpha s}\mathrm{d}s\end{array}\right\}' \tag{41}$$

Eq.(41) can be simplified as

$$F_2'(x-v_r t)=\alpha\left(F_1(0)+\beta\frac{v_r}{v_l}G_1(0)\right)\mathrm{e}^{\alpha(x-v_r t)}+\beta G_1'\left(-\frac{v_l}{v_r}x+v_l t\right)$$
$$-\alpha\left(\beta\frac{v_r}{v_l}-1\right)\left(\alpha\mathrm{e}^{\alpha(x-v_r t)}\int_0^{x-v_r t}G_1\left(-\frac{v_l}{v_r}s\right)\mathrm{e}^{-\alpha s}\mathrm{d}s+G_1\left(-\frac{v_l}{v_r}(x-v_r t)\right)\right) \tag{42}$$

By substituting Eq. (42) into Eq. (40), the energy expression for F_2 can be obtained:

$$E_{F_2}(t)_{x_1,x_2}=\rho c^2\int_{x_1}^{x_2}\left[\begin{array}{l}\alpha\left(F_1(0)+\beta\frac{v_r}{v_l}G_1(0)\right)\mathrm{e}^{\alpha(x-v_r t)}+\beta G_1'\left(-\frac{v_l}{v_r}x+v_l t\right)\\ -\alpha^2\left(\beta\frac{v_r}{v_l}-1\right)\mathrm{e}^{\alpha(x-v_r t)}\int_0^{x-v_r t}G_1\left(-\frac{v_l}{v_r}s\right)\mathrm{e}^{-\alpha s}\mathrm{d}s\\ -\alpha\left(\beta\frac{v_r}{v_l}-1\right)G_1\left(-\frac{v_l}{v_r}(x-v_r t)\right)\end{array}\right]^2\mathrm{d}x \tag{43}$$

where $E_{F_2}(t)_{x_1,x_2}$ represents the mechanical energy of the propagating wave F_2in the range of x_1 to x_2, $0<x_1<x_2<l_0$.

In the same way, the energy expressions of the propagating waves F_1, F_3, G_1, G_2 and G_3 in Fig.3 can be written as

$$E_{F_1}(t)_{x_1,x_2}=\rho c^2\int_{x_1}^{x_2}\left[F_1'(x-v_r t)\right]^2\mathrm{d}x \tag{44}$$

$$E_{F_3}(t)_{x_1,x_2}=\rho c^2\int_{x_1}^{x_2}\left[\begin{array}{l}\alpha h\mathrm{e}^{\alpha(x-v_r t)}+\beta\frac{v_r}{v_l}F_1'\left(\frac{2c}{v_l}l_0+x-v_r t\right)\\ +\alpha^2\left(\beta\frac{v_r}{v_l}-1\right)\mathrm{e}^{\alpha(x-v_r t)}\int_0^{x-v_r t}F_1\left(\frac{2c}{v_l}l_0+s\right)\mathrm{e}^{-\alpha s}\mathrm{d}s\\ +\alpha\left(\beta\frac{v_r}{v_l}-1\right)F_1\left(\frac{2c}{v_l}l_0+x-v_r t\right)\end{array}\right]^2\mathrm{d}x \tag{45}$$

where

$$h=\left(F_1(0)+\beta\frac{v_r}{v_l}G_1(0)\right)\mathrm{e}^{-\alpha\frac{v_r}{v_l}l_0}-\beta\frac{v_r}{v_l}G_1(l_0)-\beta\frac{v_r}{v_l}F_1(l_0)$$
$$-\alpha\left(\beta\frac{v_r}{v_l}-1\right)\int_0^{-\frac{v_r}{v_l}l_0}G_1\left(-\frac{v_l}{v_r}s\right)\mathrm{e}^{\alpha\left(\frac{v_r}{v_l}l_0-s\right)}\mathrm{d}s \tag{46}$$

$$E_{G_1}(t)_{x_1,x_2}=\rho c^2\int_{x_1}^{x_2}\left[G_1'(x+v_l t)\right]^2\mathrm{d}x \tag{47}$$

$$E_{G_2}(t)_{x_1,x_2}=\rho c^2\int_{x_1}^{x_2}\left[\frac{v_r}{v_l}F_1'\left(\frac{2c}{v_l}l_0-\frac{v_r}{v_l}x-v_r t\right)\right]^2\mathrm{d}x \tag{48}$$

$$E_{G_3}(t)_{x_1,x_2}=\rho c^2\int_{x_1}^{x_2}\left[\begin{array}{l}\alpha\dfrac{v_r}{v_l}\left(F_1(0)+\beta\dfrac{v_r}{v_l}G_1(0)\right)\mathrm{e}^{\alpha\left(\frac{2c}{v_l}l_0-\frac{v_r}{v_l}x-v_rt\right)}\\+\beta\dfrac{v_r}{v_l}G_1'\left(-\dfrac{2c}{v_r}l_0+x+v_lt\right)\\-\alpha^2\dfrac{v_r}{v_l}\left(\beta\dfrac{v_r}{v_l}-1\right)\mathrm{e}^{\alpha\left(\frac{2c}{v_l}l_0-\frac{v_r}{v_l}x-v_rt\right)}\int_0^{\frac{2c}{v_l}l_0-\frac{v_r}{v_l}x-v_rt}G_1\left(\dfrac{v_l}{v_r}s\right)\mathrm{e}^{-\alpha s}\mathrm{d}s\\-\alpha\dfrac{v_l}{v_r}\left(\beta\dfrac{v_r}{v_l}-1\right)G_1\left(-\dfrac{2cv_r}{v_l^{\,2}}l_0+\dfrac{v_r^{\,2}}{v_l^{\,2}}x+\dfrac{v_r^{\,2}}{v_l}t\right)\end{array}\right]^2\mathrm{d}x \quad (49)$$

5.2 The total energy of the string

5.2.1 The first time interval: $(0\le t<t_a)$

As shown in Fig.3(a), the total energy is the combination of the energy of these four propagating waves F_1, F_2, G_1, G_2 and the potential energy of the spring $E_k(t)$, which compose the displacement response of the string. So the energy of the string can be written as

$$E(t)=E_{F_1}(t)_{x_1=v_rt,x_2=l_0}+E_{F_2}(t)_{x_1=0,x_2=v_rt}+E_{G_1}(t)_{x_1=0,x_2=l_0-v_lt}+E_{G_2}(t)_{x_1=l_0-v_lt,x_2=l_0}+E_k(t) \quad (50)$$

where $E_{F1}(t)$, $E_{F2}(t)$, $E_{G1}(t)$ and $E_{G2}(t)$ are the energy of F_1, F_2, G_1 and G_2, respectively.

5.2.2 The second time interval: ($t_a\le t\le t_b$)

When $v>0$, the energy is due to the waves G_1, G_2, G_3, and F_2, as shown in Fig. 3(b). The total energy expression can be written as

$$\begin{aligned}E(t)=&E_{G_1}(t)_{x_1=0,x_2=l_0-v_lt}+E_{G_2}(t)_{x_1=l_0-v_lt,x_2=\frac{2cl_0}{v_r}-v_lt}+E_{G_3}(t)_{x_1=\frac{2cl_0}{v_r}-v_lt,x_2=l_0}\\&+E_{F_2}(t)_{x_1=0,x_2=l_0}+E_k(t)\end{aligned} \quad (51)$$

5.2.3 The third time interval: ($t_b<t\le T_0$)

In this interval, as shown in Fig. 3(d), the energy is due to the waves F_2, F_3, G_2, and G_3, i.e.

$$\begin{aligned}E(t)=&E_{F_2}(t)_{x_1=v_rt-\frac{v_r}{v_l}l_0,x_2=l_0}+E_{F_3}(t)_{x_1=0,x_2=v_rt-\frac{v_r}{v_l}l_0}+E_{G_2}(t)_{x_1=0,x_2=\frac{2c}{v_r}l_0-v_lt}\\&+E_{G_3}(t)_{x_1=\frac{2c}{v_r}l_0-v_lt,x_2=l_0}+E_k(t)\end{aligned} \quad (52)$$

So the total energy of the traveling string can be calculated using the initial conditions and Eqs.(50), (51), (52).

5.3 Numerical simulation

Fig. 6 (a) shows the curves for the total energy for a traveling string (V= 0.1, k=3 N/m) with the sping_dashpot-fixed boundary conditions and different levels of viscous damping for the first response cycles. When η = 0 Ns/m, the values of energy are almost equal at the beginning and end of the cycle, but fluctuate during the cycle. These indicate that the

energy gained by the traveling string at the downstream boundary at an instantaneous moment is not equal to the energy lost at the upstream boundary, but the total energy gained during a cycle is equal to the total energy lost. When $\eta > 0$, the energy of the traveling string system decreases in the cycle, and the larger that the viscous damping is, the more rapid is the attenuation.

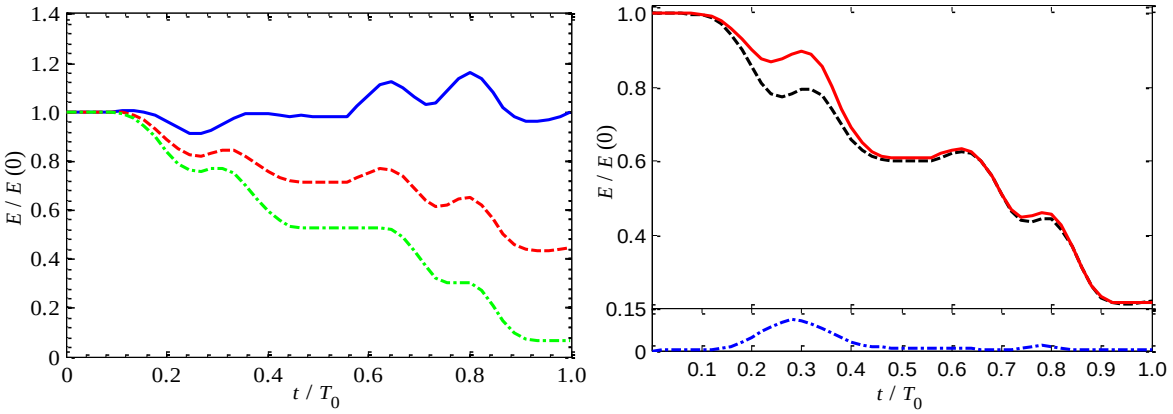

Fig. 6. The change in the transverse free vibration energy of an axially traveling string for spring -dashpot_fixed boundary conditions during the first one cycle. (a) The parameters are k = 3 N/m and non-dimensional translational speed V = 0.1. The curves are identified by viscous damping constant: —— η = 0 Ns/m, – – – η = 0.2 Ns/m, – · – η = 0.3 Ns/m. (b) The parameters are η = 0.2 Ns/m, k = 3N/m and V = 0.1. The curves are identified by: —— total mechanical energy of the axially traveling string system, – – – energy contained in all material particles of string in the region [0, L], – · – potential energy of the spring.

Fig.6 (b) shows the curves for the potential energy of the spring in a traveling string (V = 0.1, k = 3N/m, η = 0.1 Ns/m) with the spring_dashpot-fixed boundary conditions for the first response cycle. Potential energy of the spring is equal to zero at the beginning and end of the cycle, but fluctuate during the cycle. This shows that the spring acted as a store of energy during a reflection cycle. The two curves (total mechanical energy curve, curve of energy contained in the string alone) do not coincide due to the instantaneous energy stored in the spring.

When the string moves in an opposite direction, as shown in Fig. 7, the total energy attenuation of the string system for spring-dashpot_fixed boundary conditions is almost equal in one vibration period as long as the damping value is the same, regardless of whether the string translational direction is positive or negative, although the process of energy change within the period is slightly different. This means that the effect of vibration energy attenuation is the same whether the damper is placed upstream (x = 0) or downstream ($x = l_0$) as one might have expected..

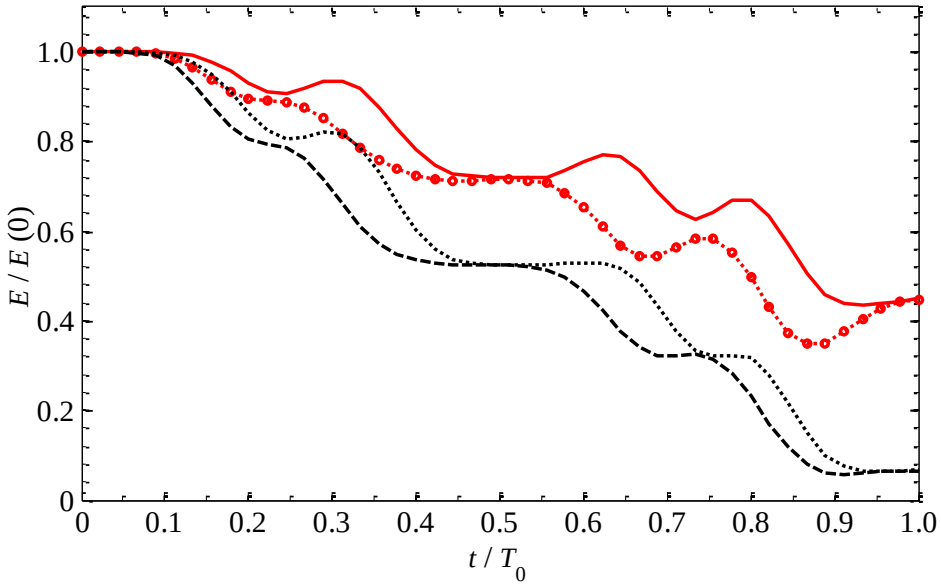

Fig.7. Comparison of vibrational energy under different damping when the string moves in opposite directions. The stiffness at the boundary is k = 3 N/m. The curves are identified by: —— V = 0.1, η = 0.1 Ns/m; ~~ooo~~ V = - 0.1, η = 0.1 Ns/m; – – – V = 0.1, η = 0.3 Ns/m; ..... V = - 0.1, η = 0.3Ns/m.

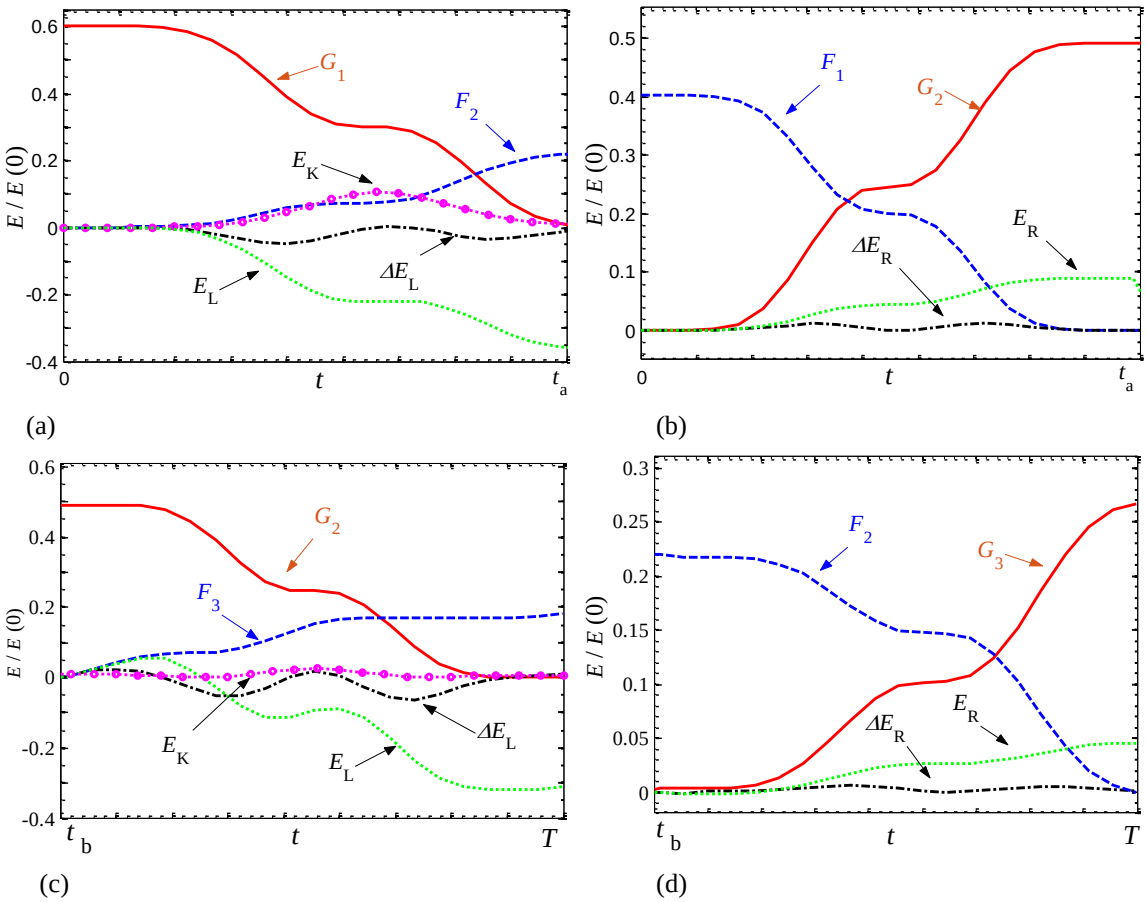

Fig.8. Variations in the energy of the propagating waves(traveling downstream F_1, F_2, F_3 and traveling upstream G_1, G_2, G_3) in a traveling string(V = 0.1) with η = 0.1 Ns/m, k = 3 N/m at the upstream boundary. The energy of the propagating waves fluctuates due to their reflections at these boundaries of

(a) $x = 0$ during the time interval $[0, t_a]$, (b) $x = l_0$ during the time interval $[0, t_a]$, (c) $x = 0$ during the time interval $[t_b, T_0]$ and (d) $x = l_0$ during the time interval $[t_b, T_0]$. E_L and E_R are the variations of energy for the traveling string due to the left boundary ($x = 0$) and the right boundary ($x = l_0$) respectively from 0 to t_a at (a) and (b) or from t_b to T at (c) and (d). E_k is the potential energy which variation energy stored in the spring through the left boundary ($x = 0$) from 0 to t_a at (a) or from t_b to T at (c). The energies of ΔE_L and ΔE_R are the instantaneous variation of change in the energy due to the left boundary ($x = 0$) and the right boundary ($x = l_0$) respectively, $\Delta E_L(i) = E_L(i) - E_L(i - 1)$ and $\Delta E_R(i) = E_R(i) - E_R(i - 1)$.

Fig.8(a), (c) show the energy changing relationships and trend amongst incident wave, reflected wave and potential energy of spring at the spring-dashpot boundary of x= 0. In Fig.8(a), the energy of G_1 decreases and the energy of F_2 increases. The potential energy of the spring E_k increases and then decreases as it stores and then releases the energy for the traveling wave. From Figs.8(a) to (d), one can see that the variations of energy E_L is less than zero and E_R is greater than zero, which indicates that the energy of the system flows out ($x = 0$) or into($x = l_0$) the string at the two boundaries respectively. As shown in Fig.8(c) and (d)，one can see that the energy gained at the right boundary is less than the energy lost at the left boundary, e.g. $E_L(T)$ = -0.31 and $E_R(T)$ = 0.045. The reason behind this phenomenon and difference is due to the viscous damper at the left boundary dissipating energy, so the overall energy of the system is reduced, as shown in the curve in Fig.6(a) marked by - - -. From ΔE_L and ΔE_R, one can judge whether the energy is flowing into (ΔE_L or $\Delta E_R > 0$) or out of (ΔE_L or $\Delta E_R < 0$) the system from the respective boundaries.

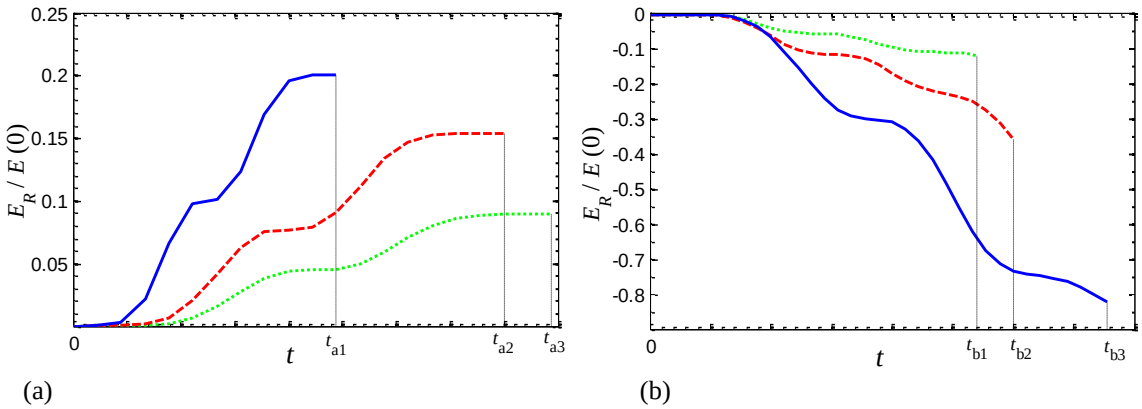

(a) (b)

Fig.9. The variations of energy for the traveling string with different values and directions for the traveling string velocity due to the right boundary ($x = l_0$) with η = 0.1 Ns/m, k = 3 N/m at left boundary. The curves are identified by: (a) - . - V = 0.1, - - - V = 0.2, —— V = 0.5; (b) - . - V = - 0.1, - - - V = - 0.2, —— V = - 0.5. The different velocity values have different t_a (t_{a1} / T_0 = 0.2, t_{a2} / T_0 = 0.4, t_{a3} / T_0 = 0.444) and t_b (t_{b1} / T_0 = 0.54, t_{b2} / T_0 = 0.6, t_{b3} / T_0 = 0.7556).

In Fig. 9, the variations of energy for the traveling string with different traveling string speed due to the right boundary, i.e. the fixed boundary at $x = l_0$, from 0 to t_a are given. The string travels with (a) positive and (b) negative speed V. Here, the conclusions for the variations in the behavior of energy at the boundary are opposite, i.e. the energy increases in case (a) and it decays in case (b). For higher string translational velocities the energy variations at the boundary will increases or decreases, for positive or negative V respectively.

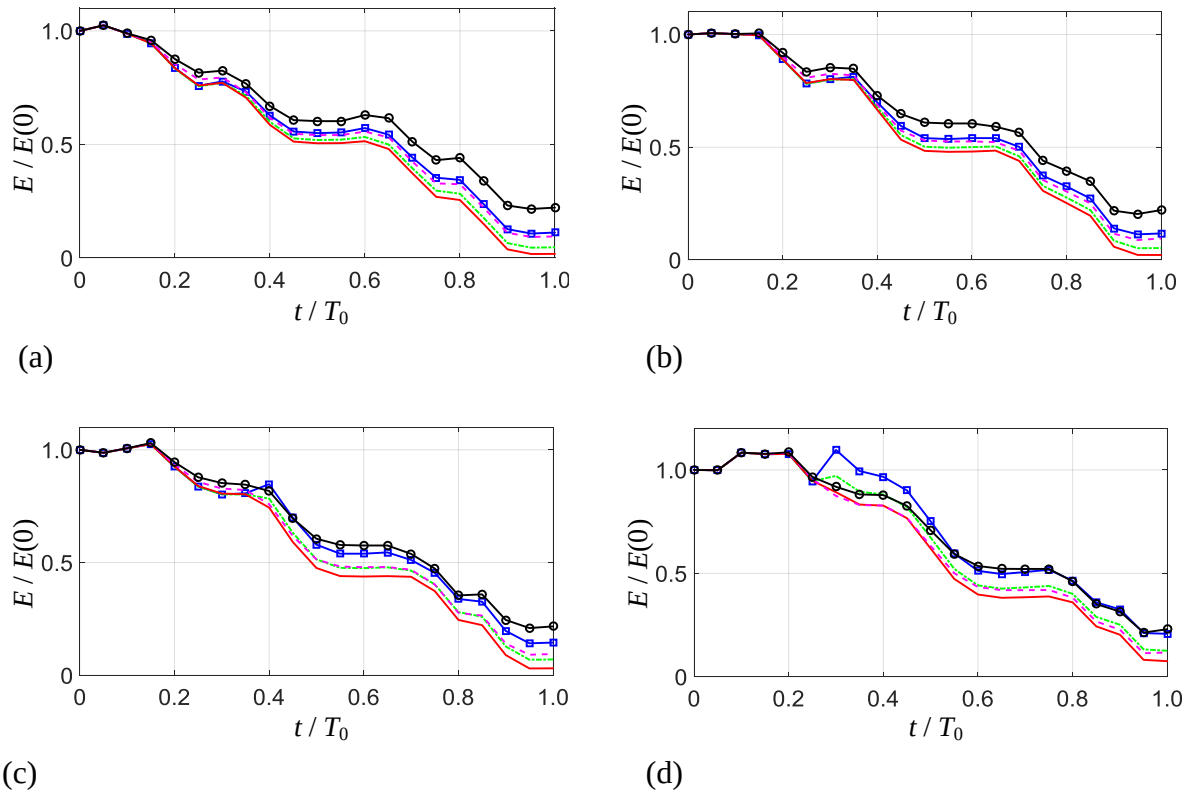

Fig.10. Energy change under different damping for traveling string with non-dimensional translational velocity of (a) $V = 0.1$, (b) $V = 0.2$, (c) $V = 0.3$ and (d) $V = 0.5$. The curves are identified by: η = 0.3, $\eta = 0.4$, $\eta = 0.55$(optimal value), $\eta = 1.0$ and $\eta = 1.5$.

In Fig. 10, the vibrational energies of traveling string with different damping and different translational velocities are compared. The rest parameters are the same as the example in Fig. 4. The optimal value of damping ($\eta = 0.55$) given by Eq. (20-2) is always the same regardless of the translational velocity. The vibrational energy of the system with the damping of optimal value drops fastest compared with other damping. After one vibration cycle, one can see in four subplots, the vibrational energies for the system with optimal damping value are almost dissipated to zero.

This section discusses the properties of vibrational energy exchange as a function of the boundaries, the level of damping and the translational velocity. It was shown that the damper lead to energy dissipation at the boundary, and the spring acted as a store of energy during a reflection cycle. Further, results studying the energy transfer of each traveling wave at the two boundaries highlight the dependence on the value of the translational velocity on the overall instantaneous vibrational energy in the string at any point in the cycle.

6. Conclusions

The vibration described by propagating waves in a finite length, mixed boundary conditions of the translating tensioned string model is considered and the reflective equations for the boundaries are derived. The vibrational response is solved by using a reflected wave superposition method. The accuracy and efficiency of the proposed method

are confirmed numerically by comparison to simulations produced using a Newmark-β method. The energy expressions with these mixed boundary conditions were obtained. The corresponding time domain curves for the exchange of energy at the boundaries was quantified. The understanding of this mechanism and of energy exchange at the boundaries was presented with potential for future vibration control implementation and design. Some conclusions can be drawn from this paper:

(1) The analytical solution for the transverse vibration of the traveling string system is obtained by using the proposed method. At low translational velocity, the results from the proposed method are consistent with the ones from the numerical method. At high translational velocity or even close to the critical velocity, the proposed method still has good stability, while the numerical method has been divergent.

(2) When there is no damping, the energy gained by the traveling string at the downstream boundary at an instantaneous moment is not equal to the energy lost at the upstream boundary, which causes the values of vibrational energy to fluctuate during a cycle. While the total energy gained during a cycle is equal to the total energy lost.

(3) A damping has the same energy dissipation capacity whether it is set upstream ($x = 0$) or downstream ($x = l_0$) of the traveling string, while the processes of energy dissipation are different.

(4) When the string travels into the fixed end (downstream), the energy of the string increases. When the string travels out of the fixed end (upstream), the energy of the string decreases. The change of the vibrational energy of string increases with the increase of the translational velocity of string.

(5) The damping set at one end of the string can dissipate the vibrational energy of the system. The optimal value damping, which can dissipate most of the vibratonal energy in one vibration cycle, is not related to the translational velocity, but to the tension and density of the string.

Acknowledgments

This work was supported by the National Natural Science Foundation of China [grant numbers 51675150 and 51305115].

References

[1] W. L. Miranker, The Wave Equation in a Medium in Motion, IBM Corp, 1960.

[2] J.A. Wickert, C.D. Mote Jr., Response and discretization methods for axially moving materials, Applied Mechanics Reviews, 44(11)(1991) 279-284.

[3] R.A. Sack, Transverse oscillations in travelling strings, British Journal of Applied Physics, 5 (6) (1954) 224-226.

[4] W.D. Zhu, Control volume and system formulations for translating media and stationary media with moving boundaries, Journal of Sound and Vibration, 254(1) (2002)189-201.

[5] L.Q. Chen, W.J. Zhao, A conserved quantity and the stability of axially moving non-linear beams, Journal of Sound and Vibration,286(3)(2005)663-668.

[6] S.Y. Lee, C.D. Mote Jr., A generalized treatment of the energetics of translating continua, part I: strings and second order tensioned pipes, Journal of Sound and Vibration, 204(5) (1997)

717-734.

[7] E.W. Chen, N.S. Ferguson, Analysis of energy dissipation in an elastic moving string with a viscous damper at one end, Journal of Sound and Vibration,333(9) (2014) 2556-2570.

[8] N.V. Gaiko, W.T. Van Horssen. On wave reflections and energetics for a semi-infinite traveling string with a nonclassical boundary support. Journal of Sound and Vibration, 370(2016)336-350.

[9] E.W. Chen, Q. Luo, N.S. Ferguson, et al. A reflected wave superposition method for vibration and energy of a travelling string, Journal of Sound and Vibration. 400 (2017) 40-57.

[10] E.W. Chen, Y.Q. He, H.Z. Wei and Y.M. Lu. A superposition method of reflected wave for moving string vibration with non-classical boundary, Journal of the Chinese Institute of Engineers, 42(4)(2019)327-332.

[11] E.W. Chen, K. Zhang, N.S. Ferguson, J. Wang, Y.M. Lu, On the reflected wave superposition method for a travelling string with mixed boundary supports, Journal of Sound and Vibration, 440(2019) 129-146.

[12] J.L. Huang, W.J. Zhou, and W.D. Zhu, Quasi-periodic Motions of High-dimensional Nonlinear Models of a Translating Beam with a Stationary Load Subsystem under Harmonic Boundary Excitation, Journal of Sound and Vibration, 462(2019) 114870.

[13] E.W. Chen, M.B. Li, N.S. Ferguson and Y.M. Lu, An adaptive higher order finite element model and modal energy for the vibration of a traveling string, Journal of Vibration and Control,25(5)(2019) 996-1007.

[14] H.H.E. Leipholz, On an extension of Hamilton's Variational Principle to nonconservative systems which are conservative in a higher sense, Ingenieur-Archiv, 47(5) (1978) 257-266.

[15] H. Benaroya and T. Wei, Hamilton's Principle for external viscous fluid–structure interaction, Journal of Sound and Vibration,238(1)(2000)113-145.

[16] C.M. Yao, R.F. Fung, C.R. Tseng, Non-linear vibration analysis of a travelling string with time-dependent length by new hybrid Laplace Transform/Finite Element Method, Journal of Sound and Vibration, 219(2) (1999) 323-337.

[17] W.A. Strauss, Partial Differential Equations: An Introduction, Wiley, New York, 1992.

[18] R.D. Swope, W.F. Ames, Vibrations of a moving thread line, Journal of the Franklin Institute, 275 (1) (1963) 36-55.

[19] C.A. Tan, S. Ying, Dynamic analysis of the axially moving string based on wave propagation, Journal of Applied Mechanics, 64 (2) (1997) 394-400.

***Declaration of Interest Statement**

Declaration of interests

☒The authors declare that they have no known competing financial interests or personal relationships that could have appeared to influence the work reported in this paper.

☐The authors declare the following financial interests/personal relationships which may be considered as potential competing interests: